PERGAMON

International Journal of Solids and Structures 39 (2002) 2857–2870

INTERNATIONAL JOURNAL OF SOLIDS and STRUCTURES

www.elsevier.com/locate/ijsolstr

Nonlinear vibration of viscoelastic laminated composite plates

Tae-Woo Kim, Ji-Hwan Kim *

School of Mechanical and Aerospace Engineering, Seoul National University, San 56-1, Shinlim-dong, Kwanak-ku, Seoul 151-742, South Korea

Received 1 November 2000; received in revised form 15 November 2001

Abstract

The dynamic behavior of laminated composite plates undergoing moderately large deflection is investigated by considering the viscoelastic properties of the material. Based on von Karman's nonlinear deformation theory and Boltzmann's superposition principle, nonlinear and hereditary type governing equations are derived through Hamilton's principle. Finite element analysis and the method of multiple scales are applied to examine the effect of large amplitude on the dissipative nature as well as on the natural frequency of viscoelastic laminated plates. Numerical experiments are performed for the nonlinear elastic case and linear viscoelastic case to check the validity of the procedure presented in this paper. Limitations of the method are discussed also. It is shown that the geometric nonlinearity does not affect the dissipative characteristics in the cases that have nonlinearity of perturbed order.

Keywords: Nonlinear vibration; Viscoelasticity; Method of multiple scales; Composite plate

1. Introduction

When polymeric matrix based composites are used for structural components such as graphite–epoxy or glass–epoxy, viscoelastic behavior is expected due to the time dependent properties of the matrix. Especially in a certain environment of high temperature and/or high moisture, the viscoelastic motion of the polymer becomes prominent and cannot be neglected in structural analysis. For more accurate prediction of the structural behavior, many researchers incorporated the time dependent property of the material into their field of studies. In this study, geometrically nonlinear analysis of a laminated composite plate undergoing moderately large deflection is carried out considering the time dependent behavior of the polymer matrix. A lot of literatures are available on the large deflection of the elastic system and most of them treat the nonlinear to linear frequency ratio at a given deflection order as a main topic. However, very few investigations have been made to account for the effects of geometric nonlinearity on the damping characteristics of structures (Sathyamoorthy, 1996). For the viscoelastic system, it is necessary to examine the variation of

* Corresponding author. Tel.: +82-2-880-7383; fax: +82-2-887-2662.
E-mail address: jwhkim@plaza.snu.ac.kr (J.-H. Kim).

0020-7683/02/$ - see front matter
PII: S0020-7683(01)00272-4

dissipative nature as well as the frequency ratio in the presence of considerable damping due to the viscoelastic material property.

There are a few studies dedicated to geometrically nonlinear analysis of a structure that consider the viscoelastic material property. Vinogradov (1985) investigated the creep phenomenon of a viscoelastic column and showed that geometrically nonlinear analysis presents no infinite increase in deflection after creep buckling, which is not the case in linear analysis. Aboudi (1991) analyzed the postbuckling behavior of viscoelastic laminated plates. The time dependent postbuckling behavior was presented, and results based on different theories of plates were compared with one another. Marques and Creus (1992) dealt with the nonlinear finite element analysis of viscoelastic composite structures considering the effect of moisture and temperature. Results show the time dependent deflection under mechanical and hygrothermal loads. Fung et al. (1996) studied the dynamic stability of a viscoelastic beam subjected to harmonic and parametric excitations simultaneously, and showed variation of stability boundaries when the nonlinear effect of deformation is included in the analysis.

In the present study, governing equations are derived from Hamilton's principle using the von Karman's nonlinear theory of plates and Boltzmann's superposition principle for linear viscoelastic constitutive law. In addition, the first-order shear deformation is considered in the displacement fields and to express the viscoelastic material properties, Prony–Dirichlet series are employed for approximation. The nonlinear and hereditary type governing equations are treated with the finite element method and method of multiple scales. Verification and limitation of the present approach are discussed by comparing results with those for nonlinear elastic and linear viscoelastic analysis. It is attempted to solve all coupled equations simultaneously, for the hereditary characteristics of the equations make it difficult to decouple the flexure motion. Numerical examples are presented and discussed as demonstrations.

2. Formulation

Fig. 1 shows the geometric configuration of a rectangular plate undergoing moderately large amplitude vibration. In the first-order shear deformation theory, the displacement fields are assumed as

$$\begin{aligned} u_1(x,y,z,t) &= u(x,y,t) + z\psi_x(x,y,t), \\ u_2(x,y,z,t) &= v(x,y,t) + z\psi_y(x,y,t), \\ u_3(x,y,z,t) &= w(x,y,t), \end{aligned} \tag{1}$$

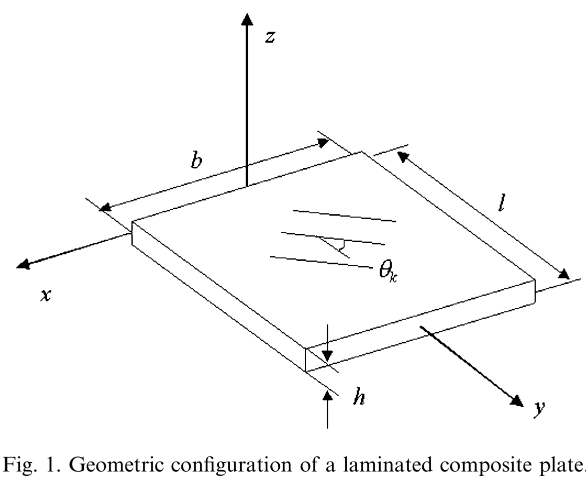

Fig. 1. Geometric configuration of a laminated composite plate.

where u_1, u_2 and u_3 are the components of the three-dimensional displacement vector in the x, y and z directions respectively, while u, v and w denote the displacements at the mid-plane, and ψ_x, ψ_y are the rotations of the normals to the mid-plane about the y and x axes.

The strain–displacement relations based on von Karman's theory of plates can be written as

$$
\begin{aligned}
\varepsilon_1 &= u_{,x} + z\psi_{x,x} + w_{,x}^2/2, \\
\varepsilon_2 &= v_{,y} + z\psi_{y,y} + w_{,y}^2/2, \\
\varepsilon_3 &= u_{,y} + v_{,x} + z(\psi_{x,y} + \psi_{y,x}) + w_{,x}w_{,y}, \\
\varepsilon_4 &= \psi_y + w_{,y}, \\
\varepsilon_5 &= \psi_y + w_{,x},
\end{aligned}
\tag{2}
$$

where contracted notations are used for engineering strains.

As the viscoelastic constitutive law, Boltzmann's superposition principle for linear viscoelastic behavior is employed. The stress–strain relation at the kth layer, which has the orientation angle of θ_k, is given in the hereditary type form as follows:

$$
\sigma_i^k(t) = \int_{0^-}^{t} \overline{Q}_{ij}^k(t-s)\dot{\varepsilon}_j^k(s)\,\mathrm{d}s, \quad i = 1, 2, \ldots, 5, \tag{3}
$$

where the repeated index stands for the summation rule, and $\overline{Q}_{ij}^k(t)$ is the relaxation function at the kth layer referred to x–y coordinates, which are obtained from the axis transformation of the relaxation modulus $Q_{ij}(t)$ referred to the principal material axes. In terms of generalized displacements and forces, constitutive relations are written in the following convolution form as in Cederbaum et al. (1991),

$$
\begin{Bmatrix} N_{xx} \\ N_{yy} \\ N_{xy} \\ M_{xx} \\ M_{yy} \\ M_{xy} \end{Bmatrix}
=
\begin{bmatrix}
A_{11} & A_{12} & A_{13} & B_{11} & B_{12} & B_{13} \\
 & A_{22} & A_{23} & B_{12} & B_{22} & B_{23} \\
 & & A_{33} & B_{13} & B_{23} & B_{33} \\
 & & & D_{11} & D_{12} & D_{13} \\
 & \text{SYM.} & & & D_{22} & D_{23} \\
 & & & & & D_{33}
\end{bmatrix}
*
\begin{Bmatrix}
\dot{u}_{,x} + w_{,x}\dot{w}_{,x} \\
\dot{v}_{,y} + w_{,y}\dot{w}_{,y} \\
\dot{u}_{,y} + \dot{v}_{,x} + \dot{w}_{,x}w_{,y} + w_{,x}\dot{w}_{,y} \\
\dot{\psi}_{x,x} \\
\dot{\psi}_{y,y} \\
\dot{\psi}_{x,y} + \dot{\psi}_{y,x}
\end{Bmatrix}
\tag{4}
$$

and

$$
\begin{Bmatrix} Q_{yy} \\ Q_{xx} \end{Bmatrix} = K \begin{bmatrix} A_{44} & A_{45} \\ A_{45} & A_{55} \end{bmatrix} * \begin{Bmatrix} \dot{\psi}_y + \dot{w}_{,y} \\ \dot{\psi}_x + \dot{w}_{,x} \end{Bmatrix},
$$

where the overdot stands for the time derivative, $*$ denotes the convolution operator and K is the shear correction factor.

Time dependent functions $A_{ij}(t)$, $B_{ij}(t)$ and $D_{ij}(t)$ are defined by

$$
\begin{aligned}
(A_{ij}(t), B_{ij}(t), D_{ij}(t)) &= \int_{-h/2}^{h/2} \overline{Q}_{ij}^k(t)(1, z, z^2)\,\mathrm{d}z \quad i, j = 1, 2, 3, \\
A_{ij}(t) &= \int_{-h/2}^{h/2} \overline{Q}_{ij}^k(t)\,\mathrm{d}z \quad i, j = 4, 5.
\end{aligned}
\tag{5}
$$

The equations of motion are derived from the extended Hamilton's principle for the nonconservative system:

$$\int_{t_1}^{t_2} (\delta T - \delta U)\,\mathrm{d}t = 0, \tag{6}$$

where δT, δU are variations of the kinetic energy and the virtual work by the internal forces respectively as are given by

$$\begin{aligned}
\delta T &= \int_{\text{Area}} \{I_0(\dot{u}\,\delta\dot{u} + \dot{v}\,\delta\dot{v} + \dot{w}\,\delta w) + I_2(\dot{\psi}_x\,\delta\dot{\psi}_x + \dot{\psi}_y\,\delta\dot{\psi}_y)\}\,\mathrm{d}x\,\mathrm{d}y, \\
\delta U &= \int_{\text{Area}} \{N_{xx}(\delta u_{,x} + w_{,x}\delta w_{,x}) + M_{xx}\,\delta\psi_{x,x} + N_{yy}(\delta v_{,y} + w_{,y}\,\delta w_{,y}) + M_{yy}\,\delta\psi_{y,y} \\
&\quad + N_{xy}(\delta u_{,y} + \delta v_{,x} + w_{,x}\,\delta w_{,y} + w_{,y}\,\delta w_{,x}) + M_{xy}(\delta\psi_{x,y} + \delta\psi_{y,x}) \\
&\quad + V_x(\delta\psi_x + \delta w_{,x}) + V_y(\delta\psi_y + \delta w_{,y})\}\,\mathrm{d}x\,\mathrm{d}y
\end{aligned} \tag{7}$$

with inertial terms I_0, I_2, resultant forces $N_{\alpha\beta}$, V_α and moments $M_{\alpha\beta}$ for $\alpha, \beta = x, y$ being defined as

$$\begin{aligned}
(I_0, I_2) &= \int_{-h/2}^{h/2} \rho(1, z^2)\,\mathrm{d}z, \\
(N_{xx}, N_{yy}, N_{xy}, V_y, V_x) &= \int_{-h/2}^{h/2} (\sigma_1^k, \sigma_2^k, \sigma_3^k, \sigma_4^k, \sigma_5^k)\,\mathrm{d}z, \\
(M_{xx}, M_{yy}, M_{xy}) &= \int_{-h/2}^{h/2} z(\sigma_1^k, \sigma_2^k, \sigma_3^k)\,\mathrm{d}z.
\end{aligned} \tag{8}$$

We again use contracted notations for stress as in the case of strain.

Interpolating displacement and rotation fields in terms of nodal values and substituting them into Eqs. (2), (3) and (6), one can obtain the following discretized nonlinear governing equations

$$\mathbf{M}\ddot{\mathbf{x}} + \sum_{i=1}^{6} \int_{0^-}^{t} Q_i(t-s)\mathbf{K}_i\dot{\mathbf{x}}\,\mathrm{d}s = 0, \tag{9}$$

where $\mathbf{x}$ is the global nodal vector, $\mathbf{M}$ is the mass matrix and $\mathbf{K}_i$ are the matrices that have stiffness Q_i as coefficients. In addition, contracted indices are used for relaxation moduli referred to the principal material axes as $Q_1 = Q_{11}$, $Q_2 = Q_{12}$, $Q_3 = Q_{22}$, $Q_4 = Q_{33}$, $Q_5 = Q_{44}$, and $Q_6 = Q_{55}$. In addition, $\mathbf{K}_1, \ldots, \mathbf{K}_4$ are transverse displacement dependent matrices, while shear deformation dependent matrices $\mathbf{K}_5$ and $\mathbf{K}_6$ are constant. They can be written as

$$\begin{aligned}
\mathbf{K}_i &= \mathbf{K}_i^0 + \mathbf{K}_i^1 + \mathbf{K}_i^2 \quad i = 1, \ldots, 4, \\
\mathbf{K}_i &= \mathbf{K}_i^0 \quad i = 5, 6,
\end{aligned} \tag{10}$$

where $\mathbf{K}_i^0$ is constant and $\mathbf{K}_i^1$, $\mathbf{K}_i^2$ are the linear and quadratic functions of transverse displacement w respectively.

3. Method of analysis

The relaxation moduli Q_{ij} referred to the principal material axes are expressed in terms of Prony–Dirichlet series, which is one of the most widely used models for approximating the viscoelastic behavior of a material. Hence, neglecting the variation of temperature and moisture, any relaxation modulus can be assumed as

$$Q_i(t) = Q_i^\infty + \sum_{j=1}^{N_i} Q_i^j \exp(-d_i^j t) = Q_i(0) f_i(t) \quad \text{for } i = 1, 2, \ldots, 6 \text{ (not summed on } i\text{)}, \tag{11}$$

where N_i is the number of exponential terms required for approximation, Q_i^∞ the final stiffness of $Q_i(t)$, Q_i^j constant coefficients, d_i^j (>0) relaxation parameters, and $f_i(t)$ is the time function that yields unity at $t = 0$ and characterizes the relaxation phenomenon.

Substituting Eq. (11) into Eq. (9), one gets a set of nondimensional equations by introducing parameters such as u/h, v/h and w/h:

$$\overline{\mathbf{M}}\ddot{\overline{\mathbf{x}}} + \frac{1}{Q_1(0)} \sum_{i=1}^{6} \int_{0^-}^{\tau} Q_i(\tau - s) \overline{\mathbf{K}}_i \dot{\overline{\mathbf{x}}} \, \mathrm{d}s = 0, \tag{12}$$

where the overbar denotes the nondimensional value. Also, nondimensional time is defined by $\tau = \omega_{\mathrm{LU}} t$ with ω_{LU} meaning the linear undamped frequency.

3.1. Linear analysis

Using the substitution method developed in Muravyov and Hutton (1997), Eq. (12) can be formulated to the eigenvalue problem through analytical evaluation of the integration term, which is made possible by introducing exponential series representation for both the relaxation moduli and solution. In other words, the solution is assumed as

$$\overline{\mathbf{x}} = \sum_{l=1}^{M(N+2)} c_l \boldsymbol{\phi}_l \exp(p_l \tau), \tag{13}$$

where M is the number of degrees of freedom, N is the total number of distinct exponential terms used in moduli approximation, $\boldsymbol{\phi}_l$ is a complex vector, and c_l, p_l are complex constants. Since $\overline{\mathbf{K}}_i$ are constant matrices in linear analysis, the integration in Eq. (12) can be calculated analytically by substituting Eqs. (11) and (13) into Eq. (12). Noting $\overline{\mathbf{K}}_i$ are constant matrices, one obtains

$$\sum_{l=1}^{M(N+2)} \left[c_l \left\{ p_l^2 \overline{\mathbf{M}} + \frac{1}{Q_1(0)} \sum_{i=1}^{6} \left(Q_i^\infty \overline{\mathbf{K}}_i + Q_i^j \overline{\mathbf{K}}_i \sum_{j=1}^{N_i} \frac{p_l}{p_l + \eta_i^j} \right) \right\} \boldsymbol{\phi}_l \exp(p_l \tau) \right] - \frac{1}{Q_1(0)} \sum_{l=1}^{M(N+2)} \sum_{i=1}^{6} \times \sum_{j=1}^{N_i} \frac{c_l p_l}{p_l + \eta_i^j} \boldsymbol{\phi}_l \exp(-\eta_i^j \tau) = \mathbf{0}, \tag{14}$$

where the relaxation parameters are normalized by the corresponding linear undamped frequency, or $\eta_i^j = d_i^j / \omega_{\mathrm{LU}}$. To satisfy Eq. (14), all coefficients of exponential functions can be set to zero to yield

$$\left\{ p_l^2 \overline{\mathbf{M}} + \frac{1}{Q_1(0)} \sum_{i=1}^{6} \left(Q_i^\infty \overline{\mathbf{K}}_i + Q_i^j \overline{\mathbf{K}}_i \sum_{j=1}^{N_i} \frac{p_l}{p_l + \eta_i^j} \right) \right\} \boldsymbol{\phi}_l = \mathbf{0} \quad l = 1, 2, \ldots, M(N+2), \tag{15.1}$$

$$\sum_{l=1}^{M(N+2)} \frac{c_l p_l}{p_l + \eta_i^j} \boldsymbol{\phi}_l = \mathbf{0} \quad j = 1, 2, \ldots, N_i \;\; i = 1, 2, \ldots, 6. \tag{15.2}$$

The eigenvalue problem is derived from Eq. (15.1) as follows. By multiplying to Eq. (15.1) a common multiple of denominators of Eq. (15.1), one gets

$$\left[\left\{p_l^2\overline{\mathbf{M}}+\frac{1}{Q_1(0)}\sum_{i=1}^{6}Q_i^{\infty}\overline{\mathbf{K}}_i\right\}\prod_{m=1}^{6}\prod_{n=1}^{N_m}(p_l+\eta_m^n)+\left\{\frac{1}{Q_1(0)}\sum_{i=1}^{6}\sum_{j=1}^{N_i}Q_i^j\overline{\mathbf{K}}_i\prod_{m=1}^{6}\prod_{n=1}^{N_m}p_l\frac{p_l+\eta_m^n}{p_l+\eta_i^j}\right\}\right]\boldsymbol{\Phi}_l$$
$$=\mathbf{0}\quad l=1,2,\ldots,M(N+1). \tag{16}$$

Denoting the matrix coefficients of $p_l^{N+2}, p_l^{N+1},\ldots,p_l^0$ in Eq. (16) as $\mathbf{B}_{N+2},\mathbf{B}_{N+1},\ldots,\mathbf{B}_0$ respectively, the eigenvalue problem equivalent to Eq. (16) is obtained as

$$\left(p_l\begin{bmatrix}\mathbf{B}_1 & \mathbf{B}_2 & \mathbf{B}_3 & \ldots & \mathbf{B}_{N+2}\\ \mathbf{I} & \mathbf{0} & \mathbf{0} & \ldots & \mathbf{0}\\ \mathbf{0} & \mathbf{I} & \mathbf{0} & \ldots & \mathbf{0}\\ \ldots & \ldots & \ldots & \ldots & \ldots\\ \mathbf{0} & \mathbf{0} & \ldots & \mathbf{I} & \mathbf{0}\end{bmatrix}+\begin{bmatrix}\mathbf{B}_0 & \mathbf{0} & \mathbf{0} & \ldots & \mathbf{0}\\ \mathbf{0} & -\mathbf{I} & \mathbf{0} & \ldots & \mathbf{0}\\ \mathbf{0} & \mathbf{0} & -\mathbf{I} & \ldots & \mathbf{0}\\ \ldots & \ldots & \ldots & \ldots & \ldots\\ \mathbf{0} & \mathbf{0} & \mathbf{0} & \ldots & -\mathbf{I}\end{bmatrix}\right)\begin{Bmatrix}\boldsymbol{\Phi}_l\\ p_l\boldsymbol{\Phi}_l\\ p_l^2\boldsymbol{\Phi}_l\\ \vdots\\ p_l^{N+1}\boldsymbol{\Phi}_l\end{Bmatrix}=\mathbf{0}. \tag{17}$$

Now, the total number of $M(N+2)$ unknowns c_l are determined by solving the following simultaneous linear equations which are composed of Eq. (15.2) and initial conditions:

$$\begin{bmatrix}\frac{p_1}{p_1+\eta_1}\boldsymbol{\Phi}_1 & \frac{p_2}{p_2+\eta_1}\boldsymbol{\Phi}_2 & \cdots & \frac{p_{M(N+2)}}{p_{M(N+2)}+\eta_1}\boldsymbol{\Phi}_{M(N+2)}\\ \cdots & \cdots & \cdots & \cdots\\ \frac{p_1}{p_1+\eta_N}\boldsymbol{\Phi}_1 & \frac{p_2}{p_2+\eta_N}\boldsymbol{\Phi}_2 & \cdots & \frac{p_{M(N+2)}}{p_{M(N+2)}+\eta_N}\boldsymbol{\Phi}_{M(N+2)}\\ \boldsymbol{\Phi}_1 & \boldsymbol{\Phi}_2 & \cdots & \boldsymbol{\Phi}_{M(N+2)}\\ p_1 & p_2 & \cdots & p_{M(N+2)}\end{bmatrix}\begin{Bmatrix}c_1\\ \vdots\\ c_{M(N+2)}\end{Bmatrix}=\begin{Bmatrix}\mathbf{0}\\ \vdots\\ \mathbf{0}\\ \overline{\mathbf{x}}(\mathbf{0})\\ \dot{\overline{\mathbf{x}}}(\mathbf{0})\end{Bmatrix}, \tag{18}$$

where the initial conditions are

$$\sum_{l=1}^{M(N+2)}c_l\boldsymbol{\Phi}_l=\overline{\mathbf{x}}(0),\qquad \sum_{l=1}^{M(N+2)}c_lp_l\boldsymbol{\Phi}_l=\dot{\overline{\mathbf{x}}}(0) \tag{19}$$

and contracted notations η_k $(k=1,2,\ldots,N)$ are used in the place of η_i^j.

3.2. Nonlinear analysis

In the geometrically nonlinear analysis, $\overline{\mathbf{K}}_i$ are no longer constant but transverse displacement dependent matrices. Generally, the relaxation develops slowly and therefore Eq. (12) is expanded in nondimensional relaxation parameters η_i^j as in Szyszkowski and Glockner (1985), and Cederbaum and Mond (1992):

$$\overline{\mathbf{M}}\ddot{\overline{\mathbf{x}}}+\frac{1}{Q_1(0)}\sum_{i=1}^{6}Q_i(0)\int_{0^-}^{\tau}\overline{\mathbf{K}}_i\dot{\overline{\mathbf{x}}}\,\mathrm{d}s+\frac{1}{Q_1(0)}\sum_{i=1}^{6}\sum_{j=1}^{N_i}\eta_i^jQ_i^j\int_{0^-}^{\tau}(\tau-s)\overline{\mathbf{K}}_i\dot{\overline{\mathbf{x}}}\,\mathrm{d}s+O(\eta^2)=0. \tag{20}$$

For the sake of brevity, some assumptions are made on the viscoelastic properties. It is assumed that Q_1 is independent of time, since the property in the longitudinal direction shows fiber dominant characteristics, and that the other moduli have the same time function $f(t)$ as in Lin and Hwang (1989). Moreover, the standard solid model, which has a single exponential term in Eq. (11) and corresponds to the $N=1$ case, is used as the time function (Chandiramani et al., 1989). Then, the time functions in Eq. (11) are written as

$$f_1(t)=1,\quad f_2(t)=f_3(t)=\cdots=f_6(t)=r+(1-r)\exp(-\eta t), \tag{21}$$

where r is the ratio of initial to final stiffness.

For the approximate solution to Eq. (20), we employ the linear elastic vibration mode as basis. According to the linear viscoelastic analysis in the previous section, there exist $N\times M$ purely dissipative modes that are damped out without vibrating, in addition to the $2M$ damped vibration mode. Furthermore, these damped vibration modes have complex values like generally damped structures because of anisotropic viscoelasticity. Therefore, this elastic mode based approach is confined to structures that show slightly viscoelastic properties. However, it is to be noted that isotropically viscoelastic structures always has the same modes as those of their elastic counterparts due to uniform distribution of damping as in Szyszkowski and Glockner (1985) and Cederbaum and Mond (1992).

Let

$$\bar{\mathbf{x}}(\tau) = \boldsymbol{\phi}\mathbf{q}(\tau), \tag{22}$$

where $\boldsymbol{\phi}$ is the lowest elastic mode shape. They are normalized to have maximum transverse deflection of unity.

Substituting Eqs. (21) and (22) into Eq. (20) and pre-multiplying it by $\boldsymbol{\phi}^{\mathrm{T}}$, one gets

$$\ddot{q} + q + \int_{0^-}^{\tau} (a_1 q + a_2 q^2)\dot{q}\,\mathrm{d}s - \eta \int_{0^-}^{\tau} (\tau - s)(a_3 + a_4 q)\dot{q}\,\mathrm{d}s + \frac{\eta^2}{2}\int_{0^-}^{\tau} (\tau - s)^2 a_3 \dot{q}\,\mathrm{d}s + \mathrm{HOT} = 0, \tag{23}$$

where $a_1, \ldots, a_4$ are constant coefficients.

The solution of Eq. (23) is sought by means of the method of multiple scales (Nayfeh, 1981). In this paper, perturbation due to nonlinearity and dissipation is parameterized by the normalized amplitude and relaxation parameter respectively, and it is assumed that the amplitude-to-thickness ratio is small and the viscoelastic behavior develops slowly. Furthermore, different time scales are introduced to obtain uniform expansions by avoiding secular terms that appear in single time scale expansions and increase infinitely with time. Now, the solution to Eq. (23) can be written as follows:

$$q(T_0, T_1, T_2, T_3, T_4, T_5, \ldots) = \varepsilon(q_1 + \varepsilon q_2 + \eta q_3 + \varepsilon^2 q_4 + \varepsilon\eta q_5 + \eta^2 q_6 + \cdots), \tag{24}$$

where ε denotes a small parameter that is a measure of the amplitude of oscillation, and different time scales are defined by

$$\begin{aligned} &\text{Order 0: } T_0 = \tau, \\ &\text{Order 1: } T_1 = \varepsilon\tau,\ T_2 = \eta\tau, \\ &\text{Order 2: } T_3 = \varepsilon^2\tau,\ T_4 = \varepsilon\eta\tau,\ T_5 = \eta^2\tau. \end{aligned} \tag{25}$$

One can see that q_3, q_5, q_6 in Eq. (24) and the time scale T_4 reflect the interaction between the large amplitude and the viscoelastic behavior. Substituting Eq. (24) into Eq. (23) and collecting terms of like powers of ε and η, the following equations are obtained through integration by parts:

$$\text{Order 1: } \varepsilon; D_0^2 q_1 + q_1 = 0, \tag{26.1}$$

$$\text{Order 2: } \varepsilon^2; D_0^2 q_2 + q_2 + 2D_0 D_1 q_1 + \frac{a_1}{2} q_1^2 = 0, \tag{26.2}$$

$$\varepsilon\eta; D_0^2 q_3 + q_3 + 2D_0 D_2 q_1 - a_3 \int_0^{\tau} q_1\,\mathrm{d}s = 0, \tag{26.3}$$

$$\text{Order 3: } \varepsilon^3; D_0^2 q_4 + q_4 + 2D_0 D_1 q_2 + 2D_0 D_3 q_1 + D_1^2 q_1 + a_1 q_1 q_2 + \frac{a_2}{3} q_1^3 = 0, \tag{26.4}$$

$$\begin{aligned} &\varepsilon^2\eta; D_0^2 q_5 + q_5 + 2D_0 D_1 q_3 + 2D_0 D_2 q_2 + 2D_0 D_4 q_1 + 2D_1 D_2 q_1 - a_3 \int_0^{\tau} q_2\,\mathrm{d}s \\ &\quad - \frac{a_4}{2}\int_0^{\tau} q_1^2\,\mathrm{d}s = 0, \end{aligned} \tag{26.5}$$

$$\varepsilon\eta^2; D_0^2 q_6 + q_6 + 2D_0 D_2 q_3 + 2D_0 D_5 q_1 + D_2^2 q_1 - a_3\left(\int_0^{\tau} q_3\,\mathrm{d}s - \int_0^{\tau}\int q_1\,\mathrm{d}s\,\mathrm{d}s\right) = 0, \tag{26.6}$$

where D_m denotes the partial derivative with respect to T_m.

One can solve Eqs. (26.1)–(26.6) in succession for $q_1, \dots, q_6$. The solution of Eq. (26.1) can be expressed in the following form:

$$q_1 = A(T_1, \dots, T_5)\exp(iT_0) + A^*(T_1, \dots, T_5)\exp(-iT_0), \tag{27}$$

where A^* means the complex conjugate of A. The detailed expression for the coefficient A on each time scale are determined from the conditions that $q_2, \dots, q_6$ have uniform expansion with respect to time. These conditions are obtained in the course of solving Eqs. (26.1)–(26.6) sequentially by eliminating terms that cause resonance:

$$D_1 A = 0, \tag{28.1}$$

$$D_2 A + \frac{a_3}{2} A = 0, \tag{28.2}$$

$$D_0 D_3 A + \frac{1}{8}\left(a_2 - \frac{5}{6}a_1^2\right)A^2 A^* = 0, \tag{28.3}$$

$$D_4 A = 0, \tag{28.4}$$

$$D_5 A + \frac{i}{2}\left(1 - \frac{3}{8}a_3\right)a_3 A = 0. \tag{28.5}$$

As a result, the dependency of A on each time scale is expressed up to the second-order times scale as follows:

$$A = \frac{A_0}{2}\exp\left(-\frac{a_3}{2}T_2\right)\exp\left[i\left\{\frac{\varepsilon^2 A_0^2}{8}\left(a_2 - \frac{5}{6}a_1^2\right)\exp(-a_3 T_2)T_3 - \frac{1}{2}\left(1 - \frac{3}{8}a_3\right)a_3 T_5 + B_0\right\}\right], \tag{29}$$

where A_0 and B_0 are real constants and determined from initial conditions. Recovering the original variable τ instead of different time scales, one obtains

$$q_1 = A_0 \exp(-\zeta\tau)\cos(\omega\tau + B_0), \tag{30.1}$$

$$q_2 = \frac{1}{12}A_0^2 a_1 \exp(-2\zeta\tau)\{\cos(2\omega\tau + 2B_0) - 3\}, \tag{30.2}$$

$$q_3 = 0, \tag{30.3}$$

where the exponential decay ratio ζ and nonlinear damped frequency ω are defined by

$$\begin{aligned} \zeta &= \frac{a_3}{2}\eta, \\ \omega &= 1 - \frac{1}{2}\left(1 - \frac{3}{8}a_3\right)a_3\eta^2 + \frac{\varepsilon^2 A_0^2}{8}\left(a_2 - \frac{5}{6}a_1^2\right)\exp(-a_3\eta\tau). \end{aligned} \tag{31}$$

From Eqs. (28.4) and (30.3), one finds that the amplitude measure parameter ε is decoupled with the relaxation parameter η. This means that dissipation characteristics are not affected by the magnitude of vibration amplitude within this expansion order. For the decay ratio in Eq. (31) is also independent of amplitude, the nonlinear effect is more to be considered for the frequency analysis rather than for the magnitude analysis in the nonlinear analysis. Coupled effect of ε and η is to be determined by investigating the dependence on higher time scales such as $\varepsilon^2\eta\tau, \varepsilon\eta^2\tau, \dots$ Thus, the linear viscoelastic analysis and geometrically nonlinear analysis can be performed separately within a certain range of ε and η, that is to be investigated in the subsequent section through examples. It is interesting to note that the decay ratio and damped frequency have linear and quadratic dependence on η respectively.

4. Numerical examples and discussion

In the finite element analysis, the 16-node Lagrangian rectangular element is employed for discretization and 5×5 meshes over the whole domain are used after a convergence study, which is omitted in this paper for brevity. In addition to the simply supported immovable boundary condition, the following material properties are used for the numerical examples:

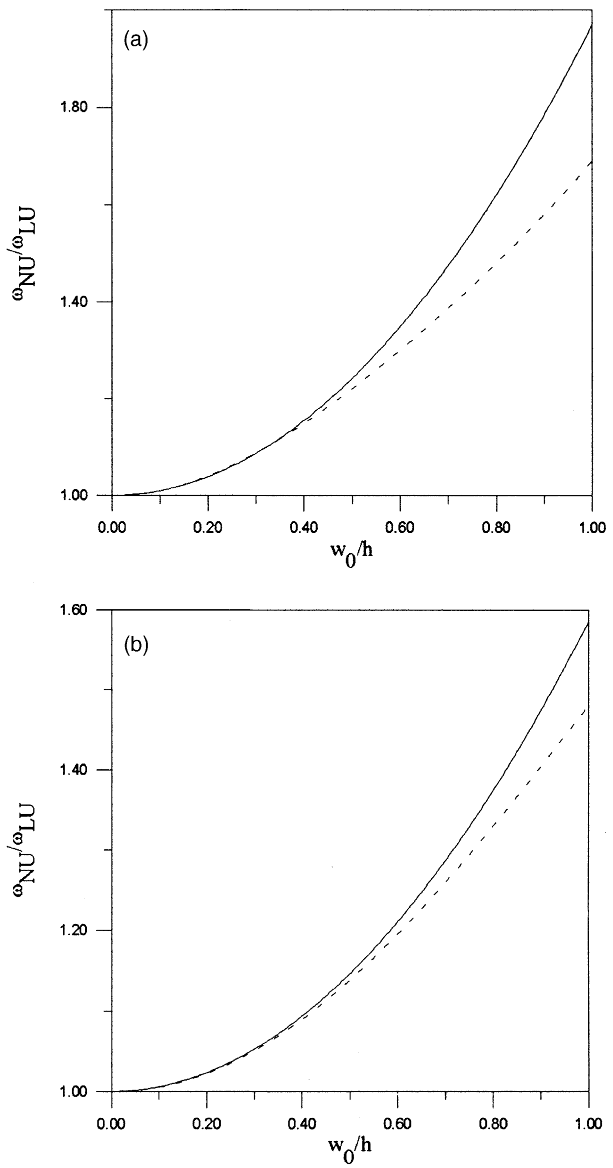

Fig. 2. Nonlinear to linear frequency ratio versus amplitude-to-thickness ratio: (a) [0°/90°], (b) [45°/−45°]; AR = 1, SR = 100, pure elastic case ($\eta = 0$), (—) present, (- - -) Singh et al.

$$E_1(0)/E_2(0) = 40, \quad G_{12}(0)/E_2(0) = G_{13}(0)/E_2(0) = 0.5, \quad G_{23}(0)/E_2(0) = 0.2, \quad \nu_{12}(0) = 0.25,$$
$$K = 5/6, \quad r = 0.4.$$

To examine the degree of error in the approximate solution Eq. (31) according to the magnitude of the small parameters, comparison work is done respectively for the elastic nonlinear case, or $\eta = 0$, in Fig. 2 and the viscoelastic linear case, or $\varepsilon \approx 0$, in Fig. 3. The fundamental nonlinear (ω_{NU}) to linear undamped frequency ratio is plotted against the amplitude-to-thickness ratio in Fig. 2 for [0°/90°] and [45°/−45 °] lay-ups, where AR and SR mean aspect ratio (l/b) and slenderness ratio (l/h) respectively. Frequency ratio is

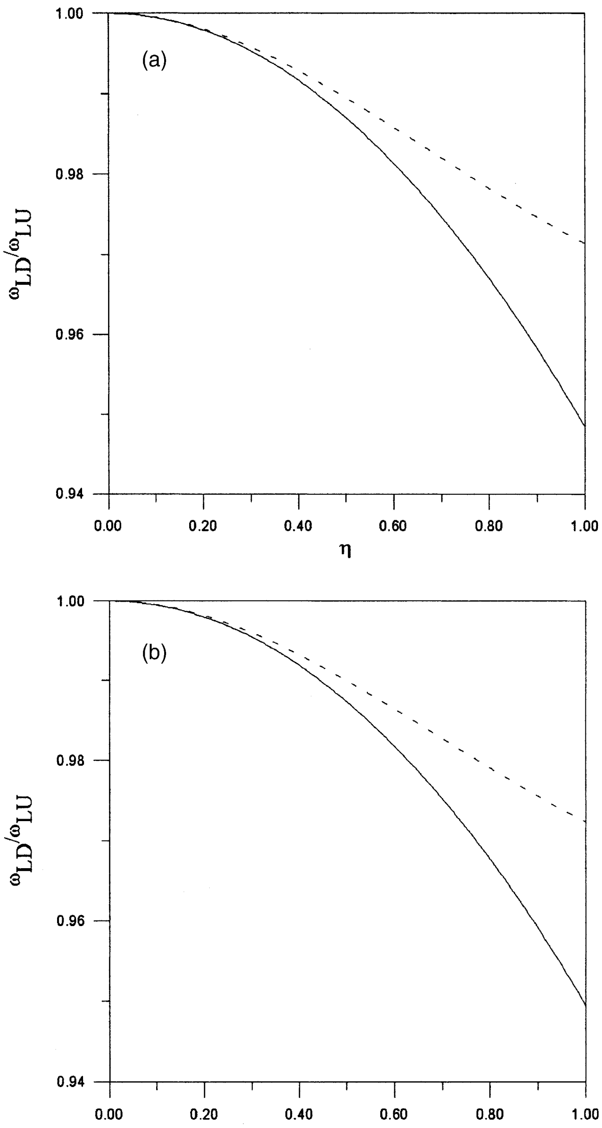

Fig. 3. Frequency reduction due to viscoelasticity: (a) [0°/90°], (b) [45°/−45°]; AR = 1, SR = 100, linear case ($\varepsilon \approx 0$), (—) present, (- - -) Eq. (17).

obtained by means of Eq. (31) in the case of $\eta = 0$, and it is compared with Singh et al. (1995), where the direct integration method is applied. It seems that at the amplitude-to-thickness ratio smaller than 0.5, the present approach gives reasonable values for both lay-ups. Frequency reduction due to viscoelastic damping is shown in Fig. 3, where the ordinate denotes ratio of linear damped (ω_{LD}) to undamped frequency. This is obtained from Eq. (31) for the viscoelastic linear case ($\varepsilon \approx 0$). To check the convergence of the results, the eigenvalue problem Eq. (17), that is applicable for general linear viscoelastic structures without limitation on the magnitude of the relaxation parameter η, is solved to obtain the linear damped frequency. Both lay-ups show similar rate of frequency change with respect to the relaxation parameter, and the results are expected to be acceptable at η smaller than 0.4 under the present expansion order. In addition, variation

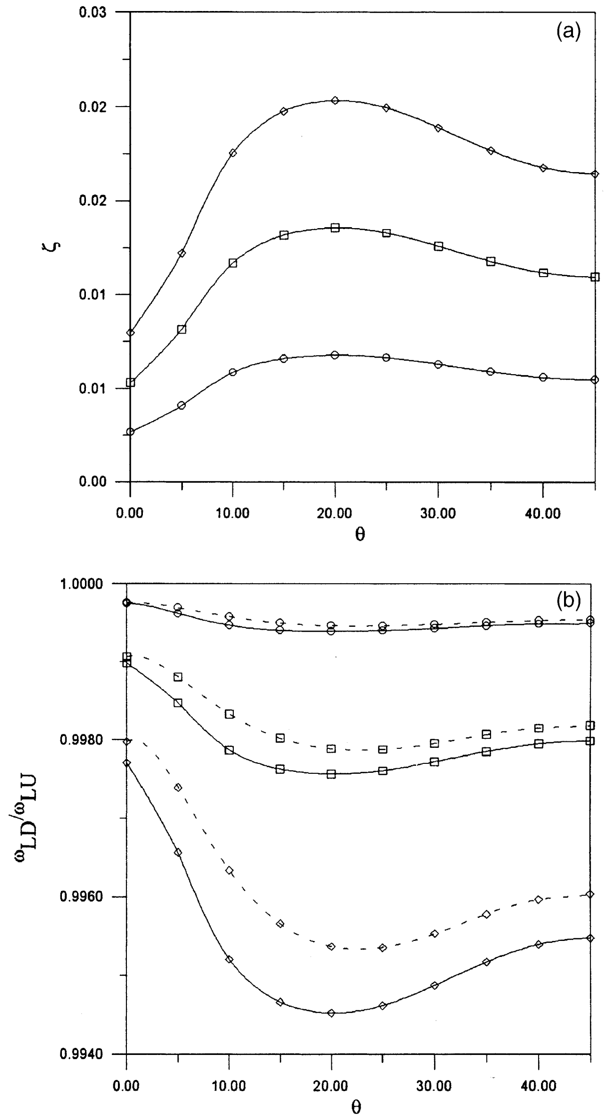

Fig. 4. Variation of decay ratio and frequency according to the layer angle: (a) decay ratio (b) frequency ratio; AR = 1, SR = 100, linear case ($\varepsilon \approx 0$), η: (○) 0.1; (□) 0.2; (◇) 0.3; (—) present, (- - -) Eq. (17).

in the decay ratio and linear damped to undamped frequency ratio are plotted respectively against the layer angle in Fig. 4 for two-layer angle plies that have the layer configuration of $[\theta°/-\theta°]$, using Eq. (31). Comparison with Eq. (17) is made for frequency only, because, as mentioned in Section 3.2, linear analysis gives $M \times N$ ($N = 1$, in these examples) more eigenvalues that are purely real and so damped out without oscillation, beside M damped vibration modes. Therefore, the decay ratio in Eq. (31) can be understood as a value that assets dissipative behavior of the same vibration mode as a whole. It is observed that the

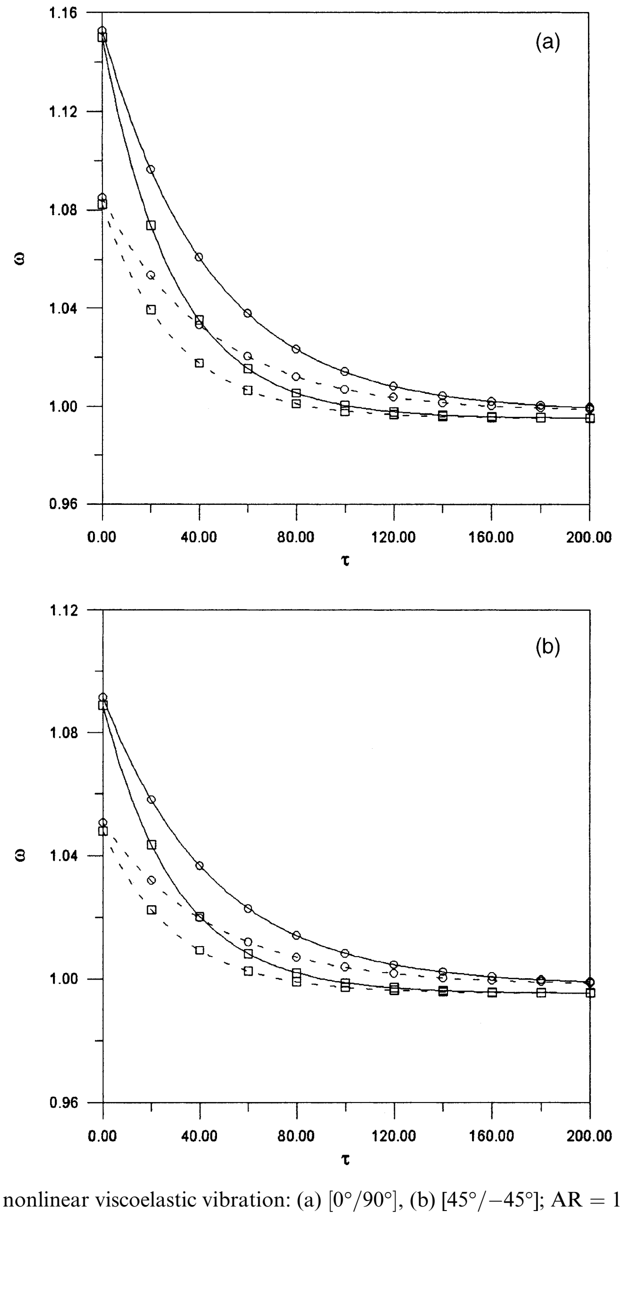

Fig. 5. Frequency history of the nonlinear viscoelastic vibration: (a) [0°/90°], (b) [45°/−45°]; AR = 1, SR = 100, w_0/h: (- - -) 0.3; (—) 0.4; η: (○) 0.2; (□) 0.3.

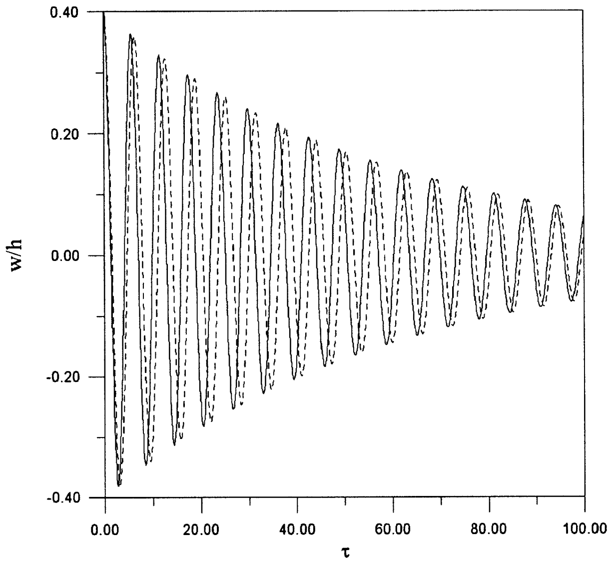

Fig. 6. Response at the central point of the plate: [0°/90°], AR = 1, SR = 100, $w_0/h = 0.4$, $\eta = 0.3$, (—) nonlinear, (- - -) linear.

dissipation nature becomes more sensitive to the layer orientation as η is increased, or the material is more viscoelastic. It is also shown that the viscoelastic effect is most remarkable around $\theta = 20°$ and least around $\theta = 0°$. In Fig. 5, the effect of nonlinearity and viscoelasticity is considered simultaneously, where ω, normalized by linear undamped frequency, is obtained from Eq. (31) for certain values of ε and η. The plates are released at $\tau = 0$ with initial transverse displacement w_0 and velocity zero. By differentiating Eq. (31) with respect to normalized time, one can easily understand that the decay rate of frequency change, or $d\omega/d\tau$, is proportional to the relaxation parameter and square of the amplitude parameter respectively. They all converge to each linear damped frequency in the long run. Finally, in Fig. 6, the response at the center point of the plate is plotted with initial conditions identical to those in Fig. 5 to emphasize that geometric nonlinearity does not affect dissipative characteristics but changes frequency only.

5. Conclusion

The viscoelastic property of the polymer was considered in geometrically nonlinear analysis of large amplitude vibration of polymeric composite plates. The effect of geometric nonlinearity on the dissipative nature was investigated by parameterizing the former as amplitude–thickness ratio and the latter as relaxation parameters respectively. It was shown that they are not coupled with each other within perturbed orders of the parameters, by deriving uncoupled solutions for a simple viscoelastic material model. In this range of the parameters, nonlinear analysis and viscoelastic analysis can be carried out separately by simply considering decaying amplitude obtained from the linear viscoelastic analysis into the conventional elastic nonlinear analysis. Therefore, nonlinear effect is more to be considered for the frequency analysis rather than for the magnitude analysis. Time dependent frequency history was also examined and the rate of change of frequency was shown to be proportional to the magnitude of the relaxation parameter and square of the maximum displacement respectively. Although a simple viscoelastic model was used for material approximation, this model can roughly simulate the time dependent behavior of polymer based composites.

Acknowledgements

This work was supported by the Brain Korea 21 project.

References

Aboudi, J., 1991. Postbuckling analysis of viscoelastic laminated plates using higher-order theory. International Journal of Solids and Structures 27 (14), 1747–1755.

Cederbaum, G., Aboudi, J., Elishakoff, I., 1991. Dynamic instability of shear-deformable viscoelastic laminated plates by Lyapunov exponents. International Journal of Solids and Structures 28 (3), 317–327.

Cederbaum, G., Mond, M., 1992. Stability properties of a viscoelastic column under a periodic force. Journal of Applied Mechanics 59, 16–19.

Chandiramani, N.K., Librescu, L., Aboudi, J., 1989. The theory of orthotropic viscoelastic shear deformable composite flat panel and their dynamic stability. International Journal of Solids and Structures 25 (5), 465–482.

Fung, R.F., Huang, J.S., Chen, W.H., 1996. Dynamic stability of a viscoelastic beam subjected to harmonic and parametric excitations simultaneously. Journal of Sound and Vibration 198 (1), 1–16.

Lin, K.Y., Hwang, I.H., 1989. Thermo-viscoelastic analysis of composite materials. Journal of Composite Material 23 (6), 554–569.

Marques, S.P.C., Creus, G.J., 1992. Geometrically nonlinear finite element analysis of viscoelastic composite materials under mechanical and hygrothermal loads. Computers and Structures 53 (2), 449–456.

Muravyov, A., Hutton, S.G., 1997. Closed-form solutions and the eigenvalue problem for vibration of discrete viscoelastic system. Journal of Applied Mechanics 64, 684–691.

Nayfeh, A.H., 1981. Introduction to Perturbation Techniques. John Wiley & Sons, New York.

Sathyamoorthy, M., 1996. Nonlinear vibrations of plates: an update of recent research developments. Applied Mechanics Review 49 (10), 55–62.

Singh, G., Rao, G.V., Iyengar, N.G.R., 1995. Finite element analysis of the nonlinear vibrations of moderately thick unsymmetrically laminated composite plates. Journal of Sound and Vibration 181 (2), 315–329.

Szyszkowski, W., Glockner, P.G., 1985. The stability of viscoelastic perfect columns: a dynamic approach. International Journal of Solids and Structures 21 (6), 545–559.

Vinogradov, A.M., 1985. Nonlinear effects in creep buckling analysis of columns. Journal of Engineering Mechanics 111 (6), 757–767.